# Tumor microenvironment as a metapopulation model : The effects of angiogenesis, emigration and treatment modalities

Halkola, Anni S.

2022-07-21

Halkola , A S , Aittokallio , T & Parvinen , K 2022 , ' Tumor microenvironment as a metapopulation model : The effects of angiogenesis, emigration and treatment modalities ' , Journal of Theoretical Biology , vol. 545 , 111147 . https://doi.org/10.1016/j.jtbi.2022.111147

http://hdl.handle.net/10138/346349
https://doi.org/10.1016/j.jtbi.2022.111147

Journal of Theoretical Biology 545 (2022) 111147

Contents lists available at ScienceDirect

Journal of Theoretical Biology

journal homepage: www.elsevier.com/locate/yjtbi

# Tumor microenvironment as a metapopulation model: The effects of angiogenesis, emigration and treatment modalities

Anni S. Halkola [a,*], Tero Aittokallio [a,b,c,d], Kalle Parvinen [a,e]

[a] Department of Mathematics and Statistics, University of Turku, Turku, Finland
[b] Institute for Molecular Medicine Finland (FIMM), University of Helsinki, Helsinki, Finland
[c] Institute for Cancer Research, Oslo University Hospital, Oslo, Norway
[d] Oslo Centre for Biostatistics and Epidemiology (OCBE), University of Oslo, Oslo, Norway
[e] Advancing Systems Analysis Program, International Institute for Applied Systems Analysis (IIASA), Laxenburg, Austria

ARTICLE INFO

*Article history:*
Received 16 September 2021
Revised 21 March 2022
Accepted 21 April 2022
Available online 27 April 2022

*Keywords:*
Anti-angiogenic treatment
Cytotoxic treatment
Combination therapy
Tumor microenvironment
Metapopulation modelling

ABSTRACT

Tumors consist of heterogeneous cell subpopulations that may develop differing phenotypes, such as increased cell growth, metastatic potential and treatment sensitivity or resistance. To study the dynamics of cancer development at a single-cell level, we model the tumor microenvironment as a metapopulation, in which habitat patches correspond to possible sites for cell subpopulations. Cancer cells may emigrate into dispersal pool (e.g. circulation system) and spread to new sites (i.e. metastatic disease). In the patches, cells divide and new variants may arise, possibly leading into an invasion provided the aberration promotes the cell growth. To study such adaptive landscape of cancer ecosystem, we consider various evolutionary strategies (phenotypes), such as emigration and angiogenesis, which are important determinants during early stages of tumor development. We use the metapopulation fitness of new variants to investigate how these strategies evolve through natural selection and disease progression. We further study various treatment effects and investigate how different therapy regimens affect the evolution of the cell populations. These aspects are relevant, for example, when examining the dynamic process of a benign tumor becoming cancerous, and what is the best treatment strategy during the early stages of cancer development. It is shown that positive angiogenesis promotes cancer cell growth in the absence of anti-angiogenic treatment, and that the anti-angiogenic treatment reduces the need of cytotoxic treatment when used in a combination. Interestingly, the model predicts that treatment resistance might become a favorable quality to cancer cells when the anti-angiogenic treatment is intensive enough. Thus, the optimal treatment dosage should remain below a patient-specific level to avoid treatment resistance.



## 1. Introduction

Cancer is a complex disease that develops and adapts uniquely in each patient and tumor. Cancer cells overcome physiological restrictions limiting the behavior of normal cells, for example, cell division, death and adaptation to hypoxic environments. Furthermore, unlike benign tumors, cancer cells are more prone to detach from the place of origin and cause metastases (Tiwari et al., 2012). These phenotypes are often caused by somatic mutations and other molecular or functional aberrations in cancer cells. The aberrant cells, or variants, may acquire survival benefits because their genetic, functional or epigenetic qualities are more suitable than those of the pre-existing main population (residents). Often these qualities are unfavorable to the patient because the cancer cells develop to become more malignant, invasive or treatment resistant. Cancer cells with these features usually form fitter populations that survive better in the dynamic evolutionary processes when competing for resources and space. A better understanding of these dynamic processes and cancer development is a key factor when trying to improve the effectiveness, personalization and precision of cancer treatment.

In addition to experimental studies, cancer development is also investigated with tools provided by mathematical modeling. Dynamic modeling has already shown promising results, including theoretical mono- or combination therapy suggestions (Halkola et al., 2020; Lai et al., 2019). Most models consider tumors that have already reached a considerable size, and thus it is justified to model the dynamics with differential equations (Fassoni et al.,

* Corresponding author at: Vesilinnantie 5, 20500 Turku, Finland.
*E-mail addresses:* ansuha@utu.fi (A.S. Halkola), tero.aittokallio@helsinki.fi (T. Aittokallio), kalle.parvinen@utu.fi (K. Parvinen).

https://doi.org/10.1016/j.jtbi.2022.111147
0022-5193/

2019; Halkola et al., 2020; Letellier et al., 2017; Pinho et al., 2013; Yonucu et al., 2017; Zhang et al., 2017). Other models start from single cells and utilize branching processes, e.g., when focusing on the early stages of primary tumor development or relapse after surgery (Avanzini and Antal, 2019; Bozic and Nowak, 2014; Kozłowska et al., 2018). Other modelling approaches, such as cellular automata (Lai et al., 2019; Alarcón et al., 2006), stochastic continuous time birth–death process (Komarova et al., 2014) and Wright-Fisher model (Fischer et al., 2015), have also been used to model cancer development and progression. However, to the best of our knowledge, there are no mathematical modelling approaches in which cancer ecosystem is considered as a continuous-time metapopulation with varying strategies.

A metapopulation is a group of populations that are spatially distinct. The populations are part of the same species and the populations are connected at some level, for example, through dispersal. The populations inhabit so-called patches, which are separate environments within the larger ecosystem. In each patch, the behavior of individuals affects the local surroundings and the living conditions. In our case, the individuals are cancer cells and the patches are possible sites for the cell subpopulations. The cancer-cell populations in a patient together constitute a metapopulation of cancer microenvironment. In the metapopulation, the cancer cells can disperse through blood and inhabit new patches, e.g., metastases, either close to the original site or further away. In general, cells do not detach easily from the extracellular matrix and survival is compromised if detached (Frisch and Screaton, 2001). However, cancer cells may utilize other mechanisms, such as epithelial-mesenchymal transition (EMT), to escape the programmed cell-death initiated after detachment (Tiwari et al., 2012). Dispersal of cancer cells may lead to inhabited patches around the body, and hence, to a metastatic disease. Dispersal also helps the cancer-cell metapopulation to survive if a local population is entirely erased by a catastrophe such as surgery.

When the cancer-cell populations grow, their resources might become insufficient if transported only through the pre-existing blood vessels. To overcome the resource restriction, cancer cells often adapt to the hypoxic surroundings or promote the formation of new vessels. The formation of new vessels, angiogenesis, is influenced by cell-secreted substances, such as vascular endothelial growth factor (VEGF) (Takahashi et al., 1995). Angiogenesis can be inhibited by anti-angiogenic treatments (Khan and Bicknell, 2016; Rajabi and Mousa, 2017; Ramjiawan et al., 2017; Shaheen et al., 1999). Such treatments target distinct inductors of angiogenesis as well as distinct benchmarks in the induction. For example, the function of VEGF can be blocked by binding to the VEGF molecule itself or to its receptors such as VEGFR2 (Bergers and Hanahan, 2008). Anti-angiogenic treatments have shown promising results both in inhibiting the tumor growth and the number of metastases (Melnyk et al., 1996; Rowe et al., 2000; Warren et al., 1995). However, anti-angiogenic treatments cannot eradicate the whole tumor or they only inhibit the tumor growth. Furthermore, anti-angiogenic treatments have less or no effect on mature, pre-existing vessels (Benjamin and Keshet, 1997), causing the resource inflow to remain at a constant level. In addition to challenges in achieving full response, tumors are prone to develop resistance to any single treatment. Anti-angiogenic treatment is not an exception since a single angiogenic mechanism can be bypassed (Bergers and Hanahan, 2008; Khan and Bicknell, 2016). Therefore, anti-angiogenic treatments have been tested in combinations with other therapies such as immunotherapy or cytotoxic treatment (Khan and Kerbel, 2018; Ramjiawan et al., 2017; Robert et al., 2011; Vasudev and Reynolds, 2014). In any case, the treatment effect is dependent on dosage and timing, thus patient-specific treatment regimens are required.

In the present work, we consider the cancer microenvironment as a metapopulation and analyze the dynamics of cancer development and treatment effects using a metapopulation model. We investigate the evolution of cancer cells with respect to changes in three evolutionary strategies: angiogenesis, emigration and treatment resistance. In particular, we investigate the effects of anti-angiogenic and cytotoxic treatment and their combinations, as well as the effect of other model parameters, such as the resource inflow and immigration rate, that affect the cell population dynamics. First, we analyze the single-strategy dynamics without treatment (Section 3.1) to provide an overview of how the different strategies evolve separately. Second, we investigate how the angiogenesis and emigration strategy evolve together (Section 3.2). Especially, we focus on the treatments effects and the changes they cause in the ecosystem both individually (Section 3.2.1) and together in a combination therapy (Section 3.2.2). Third, we bring the treatment resistance under investigation and consider all the three strategies together with the anti-angiogenic treatment to investigate how and when the resistance emerges (Section 3.3).

## 2. Materials and methods

In our metapopulation model of tumor microenvironment, cancer cells inhabit habitat patches (Fig. 1). It is assumed that there are infinitely many habitat patches, even though in reality there are eventually some restrictions when considering the sites where cells can grow. Each habitat patch has its own microenvironment and living conditions determined by the resource availability (via vasculature) and the cells living in the patch. In contrast to cellular automata, the spatial relation to other patches is not under consideration and the patches have no direct interactions or exchange. The cells can leave the patch into a dispersal pool (red rectangle in Fig. 1), which connects all patches. It is assumed that in the dispersal pool, there is no proliferation and cells may only die or immigrate into a patch. The spatial location of a patch does not affect immigration, but the population size does: Cells are more likely to immigrate into a less-populated patch since there is more space and there may be less competition for resources. The dead cells exit the system and are no longer under consideration.

### 2.1. Within-patch dynamics

#### 2.1.1. Fast within-patch resource dynamics

Resources ($R$), such as glucose, flow into and out of the patch following chemostat dynamics (Smith and Waltman, 1995). The

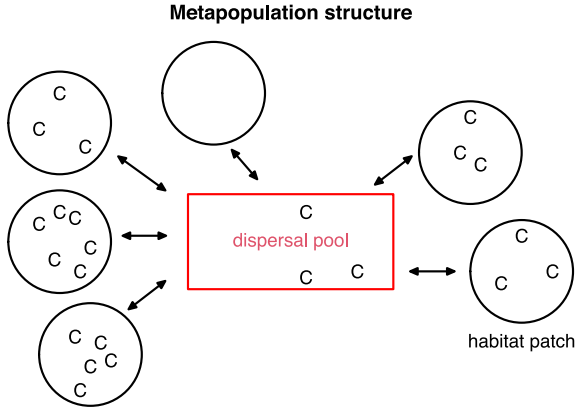


**Fig. 1.** The metapopulation structure. Black circles represent habitat patches, i.e., possible sites for cell subpopulations. The red rectangle represents the dispersal pool, i.e., the circulation system. Cells (C) may emigrate into the dispersal pool and immigrate from there into habitat patches to form metastases. (For interpretation of the references to colour in this figure legend, the reader is referred to the web version of this article.)

pre-existing vessels provide a constant resource inflow $\widehat{R}$, which is called the baseline resource inflow. If cells contribute to angiogenesis, the amount of inflowing resources increases locally by the factor $f$, which is an increasing function of the angiogenesis contribution (e.g. amount of VEGF produced). An upper bound ($A_{\max}$) is assumed for the increase because of limited space for new vessels to form in the microenvironment of a patch. Resources flow out of the patch with concentration of $R$, and both the inflow and outflow have the same relative flow speed of $\lambda$. Cells collect resources by law of mass action with their resource consumption rate (Tóth and Érdi, 1989).

Local resources follow a differential equation:

$$\frac{dR}{dt} = \lambda\left(f(\boldsymbol{n},\boldsymbol{a})\widehat{R} - R\right) - R\sum_{i=1}^{k} n_i s_i, \tag{1}$$

in which

$$f(\boldsymbol{n},\boldsymbol{a}) = \left(1 + \frac{A_{\max}\sum_{i=1}^{k} n_i a_i}{1+\sum_{i=1}^{k} n_i a_i}\right). \tag{2}$$

Here, $\boldsymbol{n} = (n_1,\ldots,n_k)$ and $\boldsymbol{a} = (a_1,\ldots,a_k)$, where $n_i$ is the number of type $i$ cells and $a_i$ is the corresponding angiogenesis strategy that tells how much cell type $i$ contributes to angiogenesis. Furthermore, $\widehat{R}$ is the baseline resource inflow, $s_i$ is the resource consumption rate of type $i$ cells, and $\lambda$ is the relative flow speed of resources. $A_{\max}$ is the upper limit of angiogenesis-increased resources inflow. It is assumed that the dynamics of local resources (1) are fast and in equilibrium (satisfying the condition $dR/dt = 0$), resulting in the resource concentration

$$R^*(\boldsymbol{n},\boldsymbol{a}) = \frac{\lambda f(\boldsymbol{n},\boldsymbol{a})\widehat{R}}{\lambda + \sum_{i=1}^{k} n_i s_i}. \tag{3}$$

When the angiogenesis strategies are zero ($a_i = 0$) or contributing cells do not exist (e.g. $a_i > 0$ but $n_i = 0$), the resource inflow is at the baseline ($\widehat{R}$).

### 2.1.2. Within-patch cancer-cell dynamics

The cell population dynamics within a patch is modelled as a continuous-time Markov chain, in which the population's state is determined by the numbers of different cell types present in the patch. The state of a local population changes when cells proliferate, die or migrate. Transitions of one cell type into another are assumed to be so rare that such transitions can be excluded from the Markov chain. It is assumed for computational reasons, and because of biological limitations of space, that a patch has a maximum limit of $K$ cells. It is assumed that cells cannot divide in a full patch with $K$ cells. The states and potential transitions of the Markov chain in a monomorphic resident population are illustrated in Fig. 2. How the probabilities of the Markov chain to be in different states change in time are given by forward Kolmogorov equations. For a monomorphic population, i.e., when all cells have the same strategy, these equations are presented in Section 2.2, Eq. (14).

Cells proliferate using collected resources and thus the birth rate depends on the resource intake. The resource availability is collectively affected by the angiogenesis contribution of all cells in the patch. Through resource usage, angiogenesis indirectly affects the birth rate. However, the angiogenesis strategy has also a direct negative effect on the birth rate since higher angiogenesis contribution reserves resources from the proliferation.

The birth rate of cell type $i$ is

$$b_{\boldsymbol{n},\boldsymbol{a},i} = \gamma s_i R^*(\boldsymbol{n},\boldsymbol{a}) g(a_i), \tag{4}$$

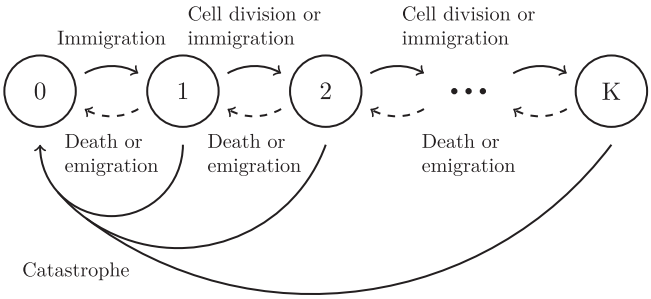


**Fig. 2.** The states and transitions of the Markov chain describing monomorphic resident population dynamics.

in which

$$g(a_i) = \frac{1}{1+a_i}. \tag{5}$$

Here, $s_i$ is the resource consumption rate, describing how much a cell type $i$ collects resources in order to divide. Cell division is proportional to the resource usage with conversion coefficient $\gamma$. The resource concentration $R^*$ is as in Eq. (3). Vectors $\boldsymbol{n}$ and $\boldsymbol{a}$ contain the numbers and angiogenesis strategies of all cell types correspondingly, and $a_i$ is the angiogenesis strategy of the cell type $i$. In addition, $g(a)$ describes the trade-off on proliferation caused by the angiogenesis contribution.

The death rate is the same for all cell types and it depends only on the total number of cells in the patch $n_T = \sum_{i=1}^{k} n_i$:

$$d_{n_T} = d_0 + \delta n_T, \tag{6}$$

where $d_0$ is the baseline death rate. It is assumed that the death rate is higher in patches with higher population size (Qiao and Farrell, 1999) and thus the factor $\delta$ is positive (and set to $1/K$). Cells may also emigrate and leave the patch with a rate of $q_i$, which depends on the emigration strategy $e_i$, describing how easily a cell detaches and leaves the patch. The emigration rate depends also on the angiogenesis strategies $a_i$, because it is assumed that emigration becomes more likely when there are more vessels through which to emigrate (Bielenberg and Zetter, 2015). Accordingly,

$$q_{\boldsymbol{n},\boldsymbol{a},e_i} = e_i f(\boldsymbol{n},\boldsymbol{a}), \tag{7}$$

where the function $f$ is given in Eq. (2). Emigrated cells die in the dispersal pool (circulation system) with the rate $\nu$. Cells in the dispersal pool encounter patches with the rate $\alpha$, and upon encounter, immigrate into the encountered patch with probability $S_n = (K-n)/K$, where $n$ is the current number of cells in the patch. Upon encounter, cells are thus more likely to immigrate into a less-populated patch. Cells compete with each other indirectly through limited resources and space.

### 2.1.3. Effect of the treatments

It is assumed that the cytotoxic treatment increases the death rate $d$ with a value of $\psi_c$. Anti-angiogenic treatment prevents angiogenesis and thus the increase in inflowing resources. It is assumed that the anti-angiogenic treatment does not decrease the inflowing resources below the baseline $\widehat{R}$. The original mature vessels are assumed to be VEGF independent and thus not affected by the anti-angiogenic treatment (Baffert et al., 2004; Gee et al., 2003). Eq. (2) is modified to include the anti-angiogenic treatment

$$f(\boldsymbol{n},\boldsymbol{a},\psi_a) = \left(1 + h(\psi_a)\frac{A_{\max}\sum_{i=1}^{k} n_i a_i}{1+\sum_{i=1}^{k} n_i a_i}\right), \tag{8}$$

with the anti-angiogenic treatment effect

$$h(\psi_a) = \frac{1}{1+\psi_a}, \tag{9}$$

where $\psi_a$ is the concentration of anti-angiogenic treatment. We note that this modification of Eq. (2) affects also the emigration rate in Eq. (7), i.e., the emigration rate decreases with the increasing anti-angiogenic treatment. It has been reported that anti-angiogenic treatment resulted in a fewer metastases when compared to untreated controls (Rowe et al., 2000; Warren et al., 1995).

*2.1.4. Resistance to the anti-angiogenic treatment*

To escape the effects of treatment, cancer cells may develop resistance to anti-angiogenic therapy (Bergers and Hanahan, 2008; Khan and Bicknell, 2016). The resistance strategy $\rho_i$ of cell type $i$ has a value between zero (no resistance) and one (full resistance). The resistance decreases the effect of anti-angiogenic treatment and allows the angiogenesis to prevail, resulting in a modified Eq. (7),

$$f(\boldsymbol{n},\boldsymbol{a},\boldsymbol{\rho},\psi_a) = \left(1 + h(\psi_a)\frac{A_{\max}\sum_{i=1}^{k} n_i a_i l(\rho_i,\psi_a)}{1+\sum_{i=1}^{k} n_i a_i}\right), \tag{10}$$

where $\rho = (\rho_1,\dots,\rho_k)$ are the resistance strategies of cell types $1,\dots,k$. Since the resistance affects the treatment, the resistance effect

$$l(\rho_i,\psi_a) = 1 + \psi_a\rho_i \tag{11}$$

is determined by the treatment function $h(\psi_a)$. Here, $l(\rho_i,\psi_a)$ is chosen such that with full resistance ($\rho_i = 1$) the treatment does not have any effect on cell type $i$. With no resistance ($\rho_i = 0$), the treatment has full effect on cell type $i$. Resistance of a cell type $i$ cancels the treatment effect only on cell type $i$.

It is assumed that acquiring and maintaining resistance requires energy. Therefore, resistance has a cost in terms of decreased birth rate. The trade-off between resistance and the birth rate is added to Eq. (4):

$$b_{\boldsymbol{n},\boldsymbol{a},i} = \gamma s_i R^*(\boldsymbol{n},\boldsymbol{a}) g(a_i,\rho_i), \tag{12}$$

where

$$g(a_i,\rho_i) = \frac{1}{1+a_i+\beta\rho_i}. \tag{13}$$

Here, $\beta$ is the trade-off factor for resistance. The trade-off factor of angiogenesis ($a_i$) is set to 1.

*2.1.5. Parameters*

The parameter values are set as in Table 1, unless otherwise mentioned. Due to large number of combinatorial possibilities, most of the parameters are kept constant in the analyses. The main focus in on the treatments, which are also the easiest to alter by an external intervention. In addition to the main analyses on the treatments, intervals for multiple parameters are investigated in the Supplement Sections 3, 5 and 6. The initial parameters in Table 1 are selected so that the metapopulation is viable without angiogenesis. An opposite case is investigated in the Supplementary Section 4. Depending on the parameter and the analysis, the parameter interval was selected such that the metapopulation becomes non-viable, or the angiogenesis strategy becomes zero, or the main trend is detected.

The cytotoxic treatment parameter is the realized effect of the drug concentration on the death rate. For real-life applications, the connection between the effect and the concentration of a specific drug (e.g., docetaxel or doxorubicin) should be determined and scaled to the model. Dose–response curves determine the cell viability in relation to the drug concentration (Wang et al., 2014; Wang et al., 2017). Dose–response curves are often formed with logistic scale for drug concentration, thus it is plausible to investigate even small changes in the effect size as the changes in the corresponding drug concentrations could be attainable. In our model the 0% cell viability (or 100% response) in dose–response curve would correspond to the effect size ($\psi_c$) that leads to non-viable metapopulation.

Since anti-angiogenic treatment does not directly cause cancer cell death, the dose–response curves are in relation to the formation of vessels (Truelsen et al., 2021). Instead of confining on a

**Table 1**
Parameters, functions and strategies used in the model. Here # denotes individuals (cells).

| Symbol | Value | Unit | Meaning |
|---|---|---|---|
| | | | *Parameters* |
| $\lambda$ | 1 | 1/timeunit | Relative flow speed of resources |
| $\widehat{R}$ | 10 | mass/volume | Baseline inflow of resources |
| $\gamma$ | 1 | 1/(mass/volume) | Resource usage conversion coefficient |
| $\mu$ | 0.01 | 1/timeunit | Rate of a catastrophe (such as surgery) |
| $s_r$ | 1 | 1/(timeunit*#) | Resource consumption rate of resident cells |
| $s_m$ | 1 | 1/(timeunit*#) | Resource consumption rate of variant cells |
| $\alpha$ | 0.2 | 1/timeunit | Immigration rate of cells |
| $\nu$ | 0.5 | 1/timeunit | Death rate of cells in circulation (dispersion pool) |
| $K$ | 10 | # | Maximum number of cells in a patch |
| $d_0$ | 0 | 1/(timeunit*#) | The baseline death rate |
| $\delta$ | $1/K$ | 1/# | Effect of population size on the death rate |
| $\psi_a$ | 0–18 | mass/volume | The concentration of anti-angiogenic treatment |
| $\psi_c$ | 0–4.5 | 1/timeunit | The effect of cytotoxic treatment |
| $A_{\max}$ | 5 | – | Maximum effect of angiogenesis |
| $\beta$ | 0.5 | - | Trade-off factor for resistance |
| $n_r$ | | # | Number of resident cells |
| $n_m$ | | # | Number of variant cells |
| | | | *Functions* |
| $f(\boldsymbol{n},\boldsymbol{a})$ | Eq. (2) | 1/timeunit | The effect of angiogenesis |
| $b_{\boldsymbol{n},\boldsymbol{a},r}$ | Eq. (4) | 1/(timeunit*#) | Birth rate of resident cells when population size is $n_T$ |
| $b_{\boldsymbol{n},\boldsymbol{a},m}$ | Eq. (4) | 1/(timeunit*#) | Birth rate of variant cells when population size is $n_T$ |
| $g(a_i)$ | Eq. (5) | - | Trade-off function of angiogenesis contribution |
| $d_{n_T,r}$ | Eq. (6) | 1/(timeunit*#) | Death rate of resident cells when population size is $n_T$ |
| $d_{n_T,m}$ | Eq. (6) | 1/(timeunit*#) | Death rate of variant cells when population size is $n_T$ |
| $q_{\boldsymbol{n},\boldsymbol{a},e_r}$ | Eq. (7) | 1/(timeunit*#) | Emigration rate of resident cells |
| $q_{\boldsymbol{n},\boldsymbol{a},e_m}$ | Eq. (7) | 1/(timeunit*#) | Emigration rate of variant cells |
| $h_{\psi_a}$ | Eq. (9) | - | The effect of anti-angiogenic treatment |
| $l(\rho_i,\psi_a)$ | Eq. (11) | - | The effect of treatment resistance |
| $p_{n_r,n_m}(t)$ | | – | Probability that a patch has $n_r$ resident and $n_m$ variant cells |
| | | | *Strategies* |
| $a_r$ | $\geqslant 0$ | 1/# | Angiogenesis strategy of resident cells |
| $a_m$ | $\geqslant 0$ | 1/# | Angiogenesis strategy of variant cells |
| $e_r$ | $\geqslant 0$ | – | Emigration strategy of resident cells |
| $e_m$ | $\geqslant 0$ | – | Emigration strategy of variant cells |
| $\rho_r$ | [0,1] | – | Resistance strategy of resident cells |
| $\rho_m$ | [0,1] | – | Resistance strategy of variant cells |

specific drug (e.g., bevacizumab), we included a simple dose–response curve (Eq. (9)), that depends on the anti-angiogenic treatment concentration $\psi_a$. To keep the model more adjustable, the concentration unit is also left unspecified as mass/volume. However, the unit could be, for example, ng/ml as in Truelsen et al. (2021).

### 2.2. Metapopulation dynamics

On the metapopulation level, we investigate the probability distribution of the number of cells in habitat patches. When the population is monomorphic, $p_n$ denotes the probability that a randomly chosen patch has $n$ cancer cells. Thus, $p_n$ must satisfy the condition $\sum_n p_n = 1$. Additionally, these probabilities satisfy the following system of differential equations (forward Kolmogorov equations):

$$\begin{aligned}
\tfrac{dp_0(t)}{dt} &= -\alpha D S_0 p_0(t) + [d_1 + q_{1,a,e}]p_1(t) + \mu\sum_{n=1}^{K} p_n(t)\\
\tfrac{dp_n(t)}{dt} &= -[\alpha D S_n + n(b_{n,a} + d_n + q_{n,a,e}) + \mu]p_n(t)\\
&\quad +[\alpha D S_{n-1} + (n-1)b_{n-1,a}]p_{n-1}(t)\\
&\quad +(n+1)[d_{n+1} + q_{n+1,a,e}]p_{n+1}(t)\,\tfrac{dp_K(t)}{dt} =\\
&\quad -[K(d_K + q_{K,a,e}) + \mu]p_K(t) + [\alpha D S_{K-1} + (K-1)b_{K-1,a}]p_{K-1}(t),
\end{aligned} \tag{14}$$

where the dispersal pool size $D$ satisfies the differential equation:

$$\frac{dD(t)}{dt} = -\left(\alpha\sum_{n=0}^{K} p_n S_n + \nu\right)D(t) + \sum_{n=1}^{K} q_{n,a,e} n p_n(t). \tag{15}$$

Here $S_n = (K-n)/K$ is the probability that a cell in the dispersal pool that has encountered a patch, actually immigrates into it. The model parameters are listed in Table 1. Note that according to (14) we have

$$\sum_{n=0}^{K}\frac{dp_n(t)}{dt} = 0 \Rightarrow \sum_{n=0}^{K} p_n(t) = \sum_{n=0}^{K} p_n(0) = C. \tag{16}$$

Since $p_n$ are probabilities, we must have $C = 1$.

#### 2.2.1. Metapopulation-dynamical steady state

In a metapopulation-dynamical steady state, the probabilities $p_n(t)$ and $D(t)$ do not depend on time, so that $p_n(t) = \bar{p}_n$ and $D(t) = \overline{D}$. The metapopulation-dynamical steady state can thus be solved from (14) and (15) with $\frac{dp_n(t)}{dt} = 0$ and $\frac{dD(t)}{dt} = 0$. Note, however, that because of (16), we need to replace one of the equations in (14) by $\bar{p}_0 + \bar{p}_1 + \cdots + \bar{p}_K = 1$. For a fixed value of $D$, the probabilities $\bar{p}_n$ can be solved from the linear system of equations

$$\begin{aligned}
0 &= -\alpha D S_0 \bar{p}_0 + [d_1 + q_{1,a,e}]\bar{p}_1 + \mu(1 - \bar{p}_0)\\
0 &= -[\alpha D S_n + n(b_{n,a} + d_n + q_{n,a,e}) + \mu]\bar{p}_n\\
&\quad +[\alpha D S_{n-1} + (n-1)b_{n-1,a}]\bar{p}_{n-1} + (n+1)[d_{n+1} + q_{n+1,a,e}]\bar{p}_{n+1}\\
1 &= \bar{p}_0 + \bar{p}_1 + \cdots + \bar{p}_K.
\end{aligned} \tag{17}$$

Let $\bar{p}_n(D)$ denote the solution of (17) for a fixed value of $D$. The equilibrium value $\overline{D}$ must then satisfy

$$1 = \frac{\sum_{n=1}^{K} q_{n,a,e} n \bar{p}_n(\overline{D})}{\left(\alpha\sum_{n=0}^{K}\bar{p}_n(\overline{D})S_n + \nu\right)\overline{D}} \tag{18}$$

derived from (15). Solutions $\bar{p}_n$ and $\overline{D}$, that satisfy both Eqs. (17) and (18) are searched numerically.

### 2.3. Evolutionary dynamics

#### 2.3.1. Variant's fitness

Cell's strategies variate randomly, for example, through point mutations in DNA. Variant cells experience the environment set by the resident population, which in this model is characterized by the distribution of different growth conditions in the patches. Invasion fitness (Metz et al., 1992) is the long-term exponential growth rate of a rare variant in the environment set by the resident. If the variant's invasion fitness in the environment defined by the resident is negative, the variant cannot invade and the variant population diminishes. Only the variants with positive invasion fitness may invade and replace the original resident, becoming a new resident. However, due to chance, even a variant with positive fitness may not be able to invade.

#### 2.3.2. Metapopulation fitness

In metapopulation models, calculating the invasion fitness is often complicated. However, the metapopulation fitness $R_{\text{metapop}}$ (Metz and Gyllenberg, 2001; Parvinen, 2011; Parvinen and Metz, 2008) is usually easier to calculate, and it can be used to determine the sign of the invasion fitness. Instead of measuring growth in real time, the metapopulation fitness measures growth between dispersal generations. It is analogous to the basic reproduction ratio $R_0$, which measures growth between actual generations, for example in the context of infectious diseases. Consider an initially small variant population in the dispersal pool. A focal variant in the dispersal pool will either die in the dispersal pool, or immigrate into a patch, in which all other cells are residents at that moment. The focal variant and all its descendants in this patch form a variant colony. As the variant population in the dispersal pool is initially small, no other variants are expected to arrive in this patch during the lifetime of the variant colony. The number of residents and variants in the patch changes according to a Markov chain (Supplementary Figs. S1 and S2). Eventually the variant colony goes extinct, i.e., the number of variants in the patch goes to zero. During its lifetime, the variant colony sends emigrants from the patch. The variant's metapopulation fitness is the expected number of variant emigrants produced by the variant colony during its lifetime. Note that the case of death of the focal variant in the dispersal pool corresponds to a variant colony of size zero without produced emigrants, and it is included in the calculation of the expected number of emigrants.

The state of the variant colony is determined by the number of residents $n_r$ and variants $n_m$ in the patch, in which $n_r \geqslant 0, n_m \geqslant 1$ and $n_r + n_m \leqslant K$. At the moment when the focal variant immigrates into the patch, there is exactly one variant, and the number of the residents depends on chance according to the resident population distribution. Therefore, the initial probability distribution of the Markov chain is

$$\begin{aligned}
\delta_0(n_r, 1) &= \frac{p_{n_r} S_{n_r}}{\sum_{n=0}^{K-1} p_n S_n}, \quad \text{for } 0 \leqslant n_r < K\\
\delta_0(n_r, n_m) &= 0, \qquad\qquad \text{for } n_m > 1
\end{aligned} \tag{19}$$

The transition intensities from the state $(n_r, n_m)$ to neighboring states are

$$\begin{aligned}
c^{0,+}_{n_r,n_m} &= n_m b_{\boldsymbol{n},\boldsymbol{a},m}, \quad \text{if } n_T = n_r + n_m < K\\
c^{0,-}_{n_r,n_m} &= n_m(d_{n_T} + q_{\boldsymbol{n},\boldsymbol{a},m})\\
c^{+,0}_{n_r,n_m} &= \alpha D S_{n_T} + n_r b_{\boldsymbol{n},\boldsymbol{a},r}, \quad \text{if } n_T = n_r + n_m < K\\
c^{-,0}_{n_r,n_m} &= n_r(d_{n_T} + q_{\boldsymbol{n},\boldsymbol{a},r}).
\end{aligned} \tag{20}$$

Here the original state is in the subscript and the superscript indicates the change in the numbers of individuals. For example, the superscript $(0,+)$ indicates that the number of residents is unchanged while the number of variants increases by one. Taking also the catastrophes into account, the transition intensity out of the state with $n_r$ residents and $n_m$ variants is

$$c_{n_r,n_m} = c^{0,+}_{n_r,n_m} + c^{0,-}_{n_r,n_m} + c^{+,0}_{n_r,n_m} + c^{-,0}_{n_r,n_m} + \mu. \tag{21}$$

The waiting time, i.e., the time that the continuous-time Markov chain spends in a state before the next transition, is exponentially distributed with parameter $c_{n_r,n_m}$. Once the transition happens, the probability that the population changes from the state $(n_r, n_m)$ to the state $(n_r, n_m+1)$ is $c^{0,+}_{n_r,n_m}/c_{n_r,n_m}$. Other transition probabilities are formed correspondingly. These transition probabilities form the transition probability matrix $P$. The probability that the Markov chain is in state $(n_r, n_m)$ after $\kappa$ transitions is $\delta^{n_r,n_m}_{\kappa}$, which can be calculated from

$$\delta_\kappa = \delta_0 P^\kappa. \tag{22}$$

We calculate the expected number of visits $w_{n_r,n_m}$ in the state $(n_r, n_m)$:

$$w = \sum_{\kappa=0}^{\infty} \delta_\kappa = \sum_{\kappa=0}^{\infty} \delta_0 P^\kappa. \tag{23}$$

The states $w_{n_r,n_m}$ with $n_m \geqslant 1$ are transient, and therefore, the expected number of visits $w_{n_r,n_m}$ are finite. Furthermore, we get (Kemeny and Snell, 1960)

$$w = \delta_0 (I - P)^{-1}, \tag{24}$$

where the matrix inverse exists for transient states. Now, $w$ can be numerically solved. Formula for the fitness is:

$$R_{\text{metapop}} = \frac{\alpha_m \sum_{n=0}^{K-1} p_n S_n}{\nu + \alpha_m \sum_{n=0}^{K-1} p_n S_n} \sum \frac{n_m q_m w_{n_r,n_m}}{c_{n_r,n_m}}, \tag{25}$$

where the transition intensity $c_{n_r,n_m}$ is as in Eq. (21). The average amount of visits $w_{n_r,n_m}$ is the component corresponding to the state $(n_r, n_m)$ in the vector (23). Here, $q_m$ is the emigration rate of variants, $p_n$ is the probability that a variant emigrant encounters a resident patch with $n$ cells, and $S_n$ is the probability that the variant actually immigrates into the patch it has encountered. The invasion fitness is positive if and only if $R_{\text{metapop}} > 1$.

#### 2.3.3. Pairwise invasibility plots

Evolutionary dynamics are illustrated using pairwise invasibility plots (PIPs) in which resident's strategy is on the horizontal axis and variant's strategy on the vertical axis. Areas where variant's fitness is negative or positive (metapopulation fitness is below one or above one) are marked with different colors (see e.g. Fig. 3a). Curves on which variant's fitness is exactly zero, are called neutral contours. They are seen as the edges between the positive and negative fitness in the PIPs. The diagonal, where the variant's strategy is equal to the resident's strategy, is a neutral contour, since the resident has a neutral fitness against itself. Depending on parameters, there can exist also other neutral contours.

#### 2.3.4. Fitness gradient and singular strategy

As the random variants keep emerging, the highest chance of successful invasion is on those variants, which have highest fitness. A variant's fitness increases the most in the direction given by the fitness gradient. In reality, the changes do not happen straight along the gradient. However, as the chances of invasion in that direction are higher, in time the strategies will evolve to the gradient's direction. The fitness gradient is calculated by differentiating the fitness function (Eq. (25)) with respect to a variant's strategy and then setting the variant's strategy to be equal to resident's strategy. In case of a multi-dimensional strategy (strategy vector), the fitness gradient is obtained in similar fashion by calculating partial derivatives with respect to each strategy (component). A variant's fitness increases the most in the direction given by the fitness gradient.

$$D(a_r, e_r, \rho_r) = \left( \frac{\partial}{\partial a_m} R_{\text{metapop}}, \frac{\partial}{\partial e_m} R_{\text{metapop}}, \frac{\partial}{\partial \rho_m} R_{\text{metapop}} \right)\Big|_{a_m=a_r, e_m=e_r, \rho_m=\rho_r}. \tag{26}$$

A point where the fitness gradient vanishes (all components become zero) is called evolutionarily singular strategy, or briefly just a singular strategy. For one-dimensional strategies, a singular strategy is attracting when near the point smaller values have a positive gradient and higher values have a negative gradient. In an opposite case, the singular strategy is repelling. A singular strategy is uninvadable (evolutionarily stable) if there is no strategy that could make an invasion. Correspondingly, a singular strategy is invadable if some other strategy could make an invasion. In a PIP, the singular strategies are positioned at the intersections of the diagonal and other neutral contours.

#### 2.3.5. Average population size and average emigration

To monitor the effect of cell strategies on the population level, average population size is calculated from the distribution of the population size, i.e. the probabilities $p_n$ from the residents steady state (Eq. (17)). Average population size is then

$$\sum_{n=0}^{K} n p_n. \tag{27}$$

Average emigration is calculated using the distribution of the population size $p_n$ with the emigration rate (Eq. (7)):

$$\sum_{n=0}^{K} p_n e f(n, a). \tag{28}$$

## 3. Results

We investigate the cancer development in the metapopulation model to gain insights into cancerous qualities (strategies) and how different treatment regimens affect these qualities. For example, when and how much cells contribute to the angiogenesis, when they become resistant, and how treatment affects the transition. We demonstrate the model dynamics regarding different strategies on their own as well as with respect to each other. We use a variant's fitness and singular strategies to determine the possible endpoints of development and to investigate changes caused by alterations in the cancer's environment (parameters). We focus especially on the parameters of anti-angiogenic and cytotoxic treatments and their relation to the strategies. See the Supplementary Sections 3 and 5 for the other parameters.

### 3.1. Single-strategy dynamics without treatment

#### 3.1.1. Angiogenesis strategy

Angiogenesis increases the birth rate of all cells indirectly, through increased availability of resources. Therefore, if there were no cost on angiogenesis, natural selection would cause the angiogenesis strategy to increase without bounds. However, there is a trade-off between the angiogenesis strategy and the cell birth rate, since angiogenesis reserves resources from proliferation, and

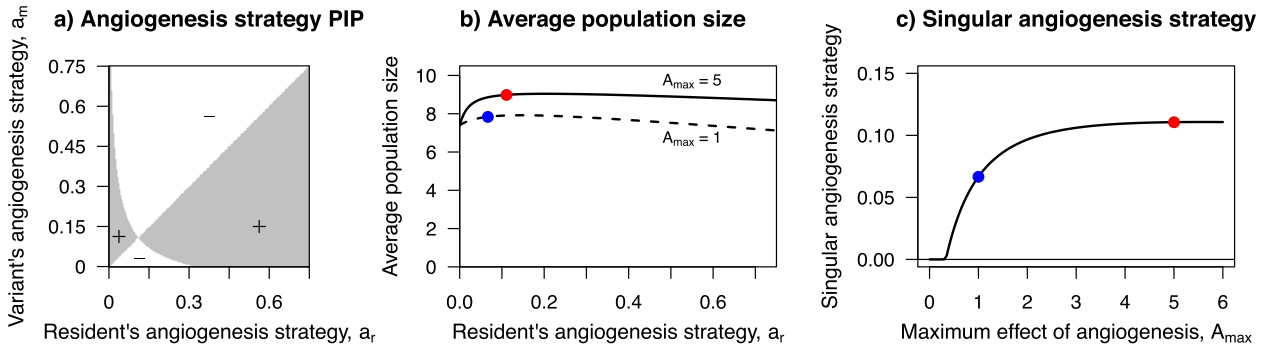


**Fig. 3.** a) Pairwise invasibility plot (PIP) for angiogenesis strategy when the emigration strategy is 0.2 and the resistance strategy is zero. b) The corresponding average population size with respect to the angiogenesis strategy for $A_{max} = 5$ (solid) and $A_{max} = 1$ (dashed). c) The singular angiogenesis strategy with respect to $A_{max}$ when the emigration strategy is 0.2 and the resistance is zero. The red dot denotes the singular strategy for $A_{max} = 5$ and the blue dot for $A_{max} = 1$. Calculation of average population size is explained in Eq. (27). Other parameters are as in Table 1. (For interpretation of the references to colour in this figure legend, the reader is referred to the web version of this article.)

therefore, higher angiogenesis directly decreases the birth rate. Despite the cost, some investment may become worthwhile to cancer cells, as can be seen from the positive singular strategy (e.g., around 0.11 in Fig. 3a). The cost of angiogenic investments (positive angiogenesis strategy) is paid by the investor itself, but benefits are obtained by all cells in the habitat, not only the cell itself. Some of them may be cell's kin. Especially, in small local populations, it is likely that some habitants are relatives and thus kin selection plays a role in evolution in this model. Depending on the relative benefits and costs, angiogenesis may evolve in the model, so that a positive singular strategy exists (Fig. 3a), in which case the positive singular angiogenesis strategy is attracting and uninvadable.

### 3.1.2. Emigration strategy

Similar to angiogenesis, kin selection affects dispersal evolution. Emigration can have direct benefits for the emigrating cell, if it arrives in a better patch than its original patch. In addition, relatives of the emigrant remaining in the original patch may benefit from an increased resource availability. Therefore, there typically exists a positive singular emigration strategy (e.g., around 0.07 in Fig. 4a). For zero or very small emigration strategy (0–0.0008 in Fig. 4a), the metapopulation is non-viable due to the positive catastrophe rate. A catastrophe can be assimilated with surgery, through which some populations are erased whereas possibly undetected metastases guarantee the survival of the cancer metapopulation. The emigration strategy is also affected by the death rate of cells in the dispersal pool. Intuitively, a higher death rate results in a decreased emigration strategy since the benefit of emigration is also decreased. However, we observe, that in our model the benefit from emigration becomes less straightforward when the death rate in the dispersal pool is increased (Fig. 4c). Eventually, the singular emigration strategy increases when the death rate in the dispersal pool is increased. Similar non-monotonic results have been reported by Comins et al. (1980), Gandon and Michalakis (1999), and Heino and Hanski (2001). Angiogenesis affects the population sizes through resources and the birth rate, and the probability of a cell finding a less-populated patch changes accordingly. On the other hand, angiogenesis also makes the emigration easier by adding vessels, and to prevent over-emigration, the emigration strategy decreases when the angiogenesis strategy is increased, if the death rate in the dispersal pool is kept constant (see the dashed curves in Fig. 5).

### 3.1.3. Resistance strategy

Without treatment, cells do not benefit from the treatment resistance, so that there are only costs, because of the trade-off with birth rate. In this case, the resistance strategy evolves to zero. Thus, there is no positive singular resistance strategy without treatment (see Supplementary Section 2).

## 3.2. Joint evolution of angiogenesis and emigration in the absence of treatment resistance

Among the three strategies, we focus first on the angiogenesis and emigration strategies and how those evolve and affect the pop-

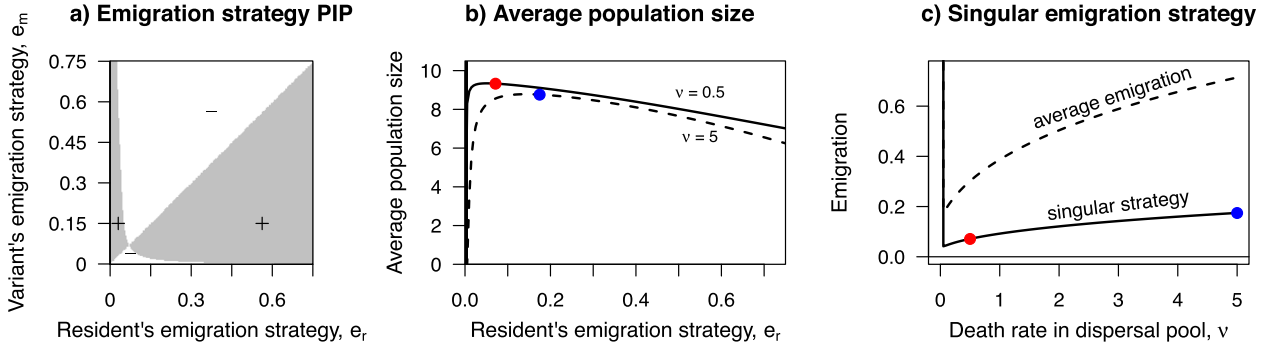


**Fig. 4.** a) PIP for emigration strategy when the angiogenesis strategy is 0.2 and the resistance strategy is zero. For smaller values (0–0.0008), the population is non-viable. b) The corresponding average population size with respect to emigration strategy for $v = 0.5$ (solid) and $v = 5$ (dashed). c) The singular emigration strategy (solid) and the average emigration rate (dashed) with respect to $v$ when the angiogenesis strategy is 0.2 and the resistance is zero. Calculation of average emigration is explained in Eq. (28). The red dot denotes the $v = 0.5$ and the blue dot denotes $v = 5$. Calculation of average population size is explained in Eq. (27). Other parameters are as in Table 1.

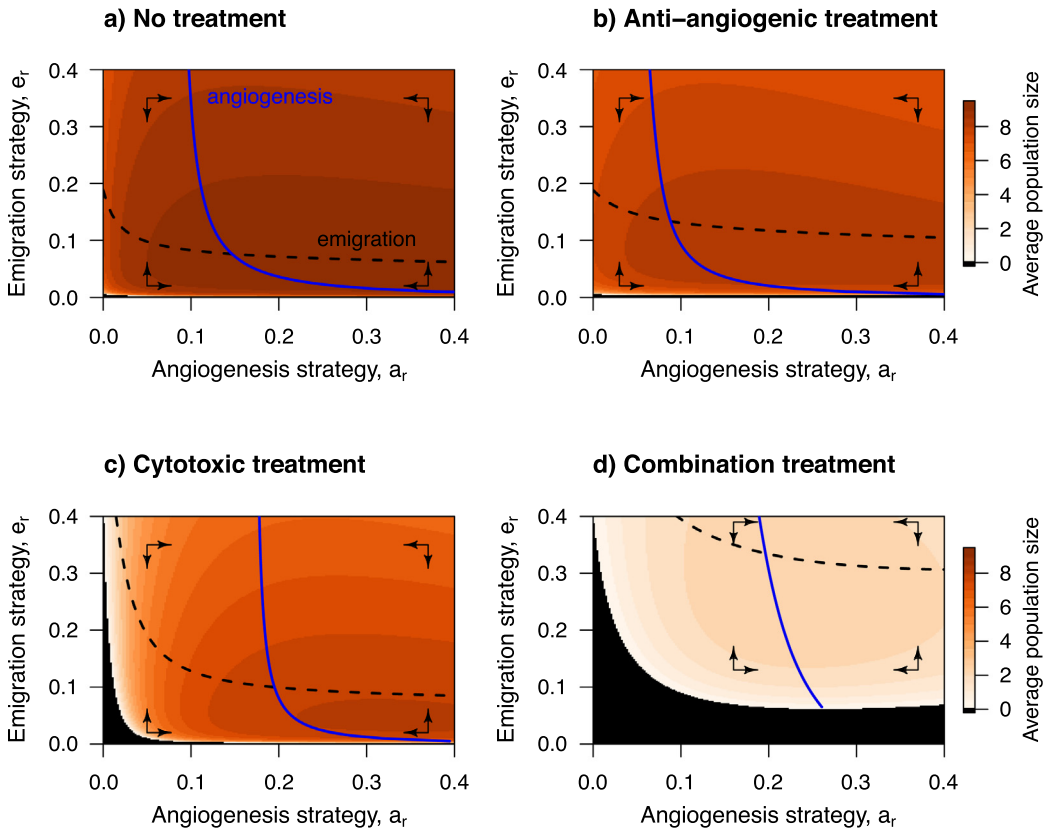


**Fig. 5.** The zero-contour curves of the components of the fitness gradient (blue curve for the angiogenesis strategy, black dashed curve for the emigration strategy). The intersection of these two curves is the singular strategy of joint evolution of angiogenesis and dispersal. Arrows show the direction of the components of the fitness gradient. The average population size is presented as a heatmap for each strategy combination. a) No treatment is used. Only b) anti-angiogenic (with concentration 3) or c) cytotoxic treatment (with effect size of 1.5). d) Combination of anti-angiogenic (concentration 3) and cytotoxic (effect size 1.5) treatment. Other parameters are as in Table 1.

ulation. In Figs. 3 and 4, the strategy dynamics were investigated separately, but more interesting is how those two strategies evolve together. A change in either of the strategies shifts the fitness landscape, and consequently also the fitness gradient. The direction of the fitness gradient (angiogenesis and emigration components) are illustrated in Fig. 5 for different treatment options. Especially, solid and dashed curves illustrate such strategy vectors, for which one component of the fitness gradient is zero. These zero-contour curves are thus singular strategies of one-dimensional strategy dynamics of the corresponding component, when other strategy components are kept constant. We observe that the zero-contour curve corresponding to each strategy component is a decreasing function of the other strategy component, so that increasing one component makes the other one less favorable to cancer cells. In these phase-plane plots, the intersections of the contour curves mark the singular strategies of vector-valued strategy evolution. These attractors do not necessarily maximize the average population size (shades of red and orange color in Fig. 5), because the best interest for an individual is not necessarily the best for the population. This phenomenon can be observed also when only a single strategy is investigated (see, e.g., Fig. 3a vs. 3b). The attractor of strategy dynamics, and hence the average population size, is affected by the microenvironment and the parameters defining it. The treatment parameters are the easiest to alter by external interventions, and therefore we focus on those in the next subsections.

*3.2.1. Cytotoxic treatment leads to non-viability, anti-angiogenic treatment decreases population size*

Cytotoxic treatment increases the death rate and thus decreases the average population size. Cancer cells tend to be more related in smaller populations. Through kin selection, such circumstances favor cooperative strategies, such as angiogenesis. Similarly, higher emigration strategy is expected to evolve because, due to the treatment, cells are more likely to find less-populated patches. In addition, emigrating cells will leave more resources for their relatives. When considering the evolution of the two strategy components separately, increasing the cytotoxic treatment is expected to increase the singular strategies. However, as we observed above, the zero-contour curve of each component of the fitness gradient is a decreasing function of the other strategy component (Fig. 5). Therefore, when considering the joint evolution of the two strategy components, increasing the cytotoxic treatment could increase one strategy component while the other one decreases due to indirect effects. However, the direct effects of increasing the cytotoxic treatment dominate, and in the joint singular strategy, both strategy components increase (Fig. 6a). Initially, the average emigration rate, and possibility of metastases, increases when cytotoxic treatment effect is increased. However, if the treatment effect is further increased, the average emigration rate decreases as fewer and fewer cells are contributing to angiogenesis. Eventually, when the average population size approaches zero, the average emigration rate becomes equal to the emigration strategy due to the lack of angiogenesis-contributing cells. Regardless of the evolutionary response in the angiogenesis and emigration strategies, the population becomes eventually non-viable when the cytotoxic treatment is high enough (around 4.25 in Fig. 6a).

The anti-angiogenic treatment decreases the benefits of angiogenesis for the cancer population. As a result, increasing the anti-angiogenic treatment at least initially causes the singular angiogenesis strategy to decrease (Fig. 6b). High levels of angiogenesis

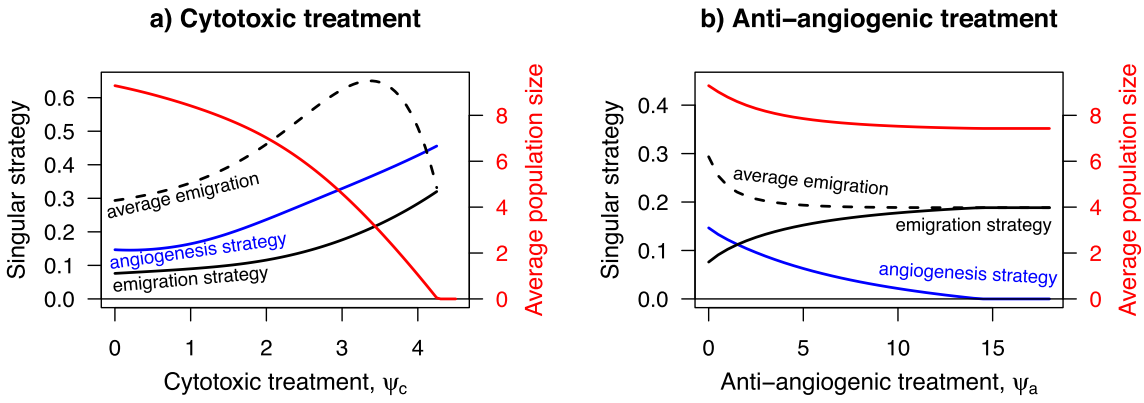


**Fig. 6.** The singular strategies of both angiogenesis strategy (blue curve) and emigration strategy (black curve) as a function of the treatment parameters. The average emigration rate is marked with black dashed line. The average population size is marked on the right-hand side y-axis with red. a) Cytotoxic treatment. b) Anti-angiogenic treatment. Other parameters are as in Table 1.

are unwanted, because they may lead into increased tumor sizes and metastases. The decrease in angiogenesis decreases the emigration opportunities. If the emigration strategy would remain the same, this would cause the average emigration rate to decrease. However, the decreased angiogenesis causes the singular emigration strategy to increase, which has an increasing effect on the average emigration rate. Nevertheless, the combined effect of these two is that the average emigration rate decreases. Eventually, if the concentration of anti-angiogenic treatment is high enough (e.g., approximately 14.5 in Fig. 6b) the singular angiogenesis strategy is pushed to zero, after which an additional anti-angiogenic treatment may not be beneficial enough for the patient. The treatment effect on the average emigration rate and the singular emigration strategy also abates, since the microenvironment is no longer affected by the anti-angiogenic treatment when the angiogenesis strategy is zero. For the same reason, the average emigration rate becomes equal to the singular emigration strategy. Unlike the cytotoxic treatment, the anti-angiogenic treatment does not necessarily lead to non-viability. The cancer population is viable even with high doses of anti-angiogenic treatment, if there is sufficient baseline resource inflow $\hat{R}$ that keeps the population viable even without angiogenesis (see Supplementary Section 4 for the case where $\hat{R}$ is insufficient).

In addition to treatments, the microenvironment is affected also by other, more internal parameters, that cannot be easily altered by external interventions. Such a parameter is, for example, the maximum effect of angiogenesis ($A_{\max}$) (see Supplementary Fig. S8f). Effects of other parameters listed in Table 1 are investigated in Supplementary information (Fig. S8).

### 3.2.2. Anti-angiogenic treatment reduces the need of cytotoxic treatment

As noted in Section 3.2.1, adding enough cytotoxic treatment leads to non-viability in the metapopulation, whereas the anti-angiogenic treatment alone decreases the average population size to some extent only. However, cytotoxic treatment has often severe side-effects and it is therefore preferable to use it at minimal effective doses. We therefore investigated whether combining these two treatments could compensate the downsides of the monotherapies.

When cytotoxic treatment is increased, the population eventually becomes non-viable regardless of the angiogenesis (or emigration) strategy. Fig. 7 illustrates that the value of $\psi_c$ for which the population becomes non-viable depends on the strategy of the population. Strategy evolution keeps the population viable for larger values of $\psi_c$ compared with a situation in which strategies would be fixed. If the strategy dynamics is fast enough, the population quickly adapts to the added treatment, and the strategy of the population will be close to the singular strategy corresponding to the current treatment level. The minimal cytotoxic treatment needed for non-viability is the value of $\psi_c$ for which the population is not viable for any strategy, i.e., the value for which the singular strategy collides with the viability boundary (the blue curve meets the black area in Fig. 7a for $\psi_c \approx 4.26$). The anti-angiogenic treatment lowers the need for the cytotoxic treatment as the edge of non-viability is reached with smaller $\psi_c$ (Fig. 7a vs. 7b). However, as noted in Section 3.2.1, increasing the anti-angiogenic treatment too much has not much benefit for the patient when already intermediate levels of treatment have caused the angiogenesis strategy to evolve close to zero. Thus, it is important to consider whether the additional anti-angiogenic therapy is worth the negligible benefit. An almost equal benefit could be reached with much lower dose of angiogenic treatment. For example, the black curve in Fig. 7c illustrates that anti-angiogenic treatment concentration of 6 requires the effect size of 1.64 of cytotoxic treatment for the population to be non-viable. With anti-angiogenic treatment concentration of 3, the required effect size of cytotoxic treatment is 1.88, which is still less than half of the effect of cytotoxic treatment needed without the anti-angiogenic treatment (4.26).

The positive treatment effects are counterbalanced by costs, such as side-effects or treatment expenses money-wise. Even if generally well tolerated with manageable side-effects (e.g., hypertension) (Rajabi and Mousa, 2017), anti-angiogenic treatment may also cause severe side-effects, such as bleeding complications and gastrointestinal perforation (Elice and Rodeghiero, 2012; Saif et al., 2007). At some point, the side-effects may become too severe for the patient to tolerate and the treatment benefit is outweighted by the negative effects. Selected cost examples are presented in Fig. 7c, illustrating that non-viability with minimal costs is obtained by combined therapy with moderate treatment levels.

### 3.3. Treatment resistance

Angiogenesis does not depend only on a single mechanism, and cancer cells may bypass such anti-angiogenic treatment mechanisms that inhibit only one target on the angiogenesis pathway (Bergers and Hanahan, 2008; Khan and Bicknell, 2016). The initial response to the anti-angiogenic treatment may be then followed by treatment resistance and eventual relapse. Next, we consider the dynamics of resistance strategy together with the angiogenesis and emigration strategies. Especially, we investigate how the concentration of anti-angiogenic treatment affects the evolution of treatment resistance.

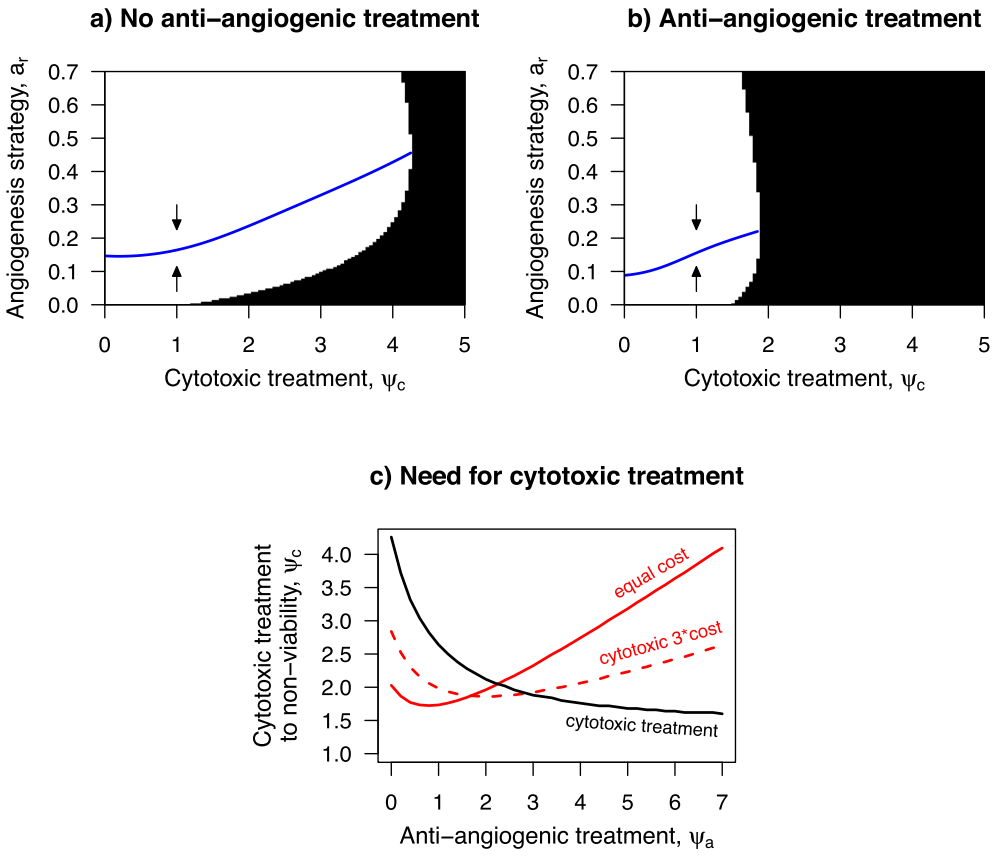


**Fig. 7.** (a-b) The singular angiogenesis strategy as a function of the cytotoxic treatment (a) without anti-angiogenic treatment (b) with anti-angiogenic treatment (concentration 3). The emigration strategy is expected to be on the corresponding singular strategy. Black region marks the non-viability. c) The minimal cytotoxic treatment needed for non-viability (black line) when the angiogenesis and emigration strategies adapt to match the treatment. The red lines (solid and dashed) illustrate the cost of treatment, e.g., in relation to treatment expenses or side-effects. The solid line: both treatments have an equal cost. The dashed line: the cytotoxic treatment has three times the cost of the anti-angiogenic treatment. Other parameters are as in Table 1.

*3.3.1. Bistability scenario in which only radical variations may lead to treatment resistance*

Consider the virtual patient with default parameters under anti-angiogenic treatment only. For small concentrations of anti-angiogenic treatment (0–3.8 in Fig. 8a), there exists a single evolutionarily attracting singular strategy, in which the resistance strategy component is zero. At higher levels of treatment, there is an additional attracting singular strategy with positive resistance, as well as a saddle point between the two attractors. This saddle point is a singular strategy, which from most directions is not evolutionarily attracting. The stable manifold of the saddle point determines for the two attractors their basins of attraction. They are areas in the strategy space from which the strategies evolve either to the singular strategy with a positive resistance or to the one with zero resistance. As illustrated by Fig. 8e, the resistance strategy component has a negative fitness gradient at zero if it is assumed that the angiogenesis and emigration strategy components are at their joint singular strategy corresponding to the current treatment (e.g., red dot in Fig. 10a for anti-angiogenic treatment 7). Since zero is the lower boundary for the resistance strategy, variants with a small positive resistance strategy component cannot invade, and the resistance strategy thus remains zero. However, as illustrated by the region of positive fitness in Fig. 8e, some variants with multiple radical variations could invade. One such invasion could then result in dynamics towards the positive singular strategy even with small variations (Fig. 8f). Fig. 8d suggests that around 3.8 is the dosage that has the maximum effect without a high risk of resistance. A higher treatment concentration would ideally lead to a lower tumor sizes (Fig. 8d). However, in the case the treatment resistance emerges, the tumor sizes increase above the level achieved with the treatment concentration of 3.8. Even though the model suggests that the resistance is not easily acquired for the virtual patient in Fig. 8, the possibility is still there.

*3.3.2. Even small variations may lead to treatment resistance*

The situation depicted in Section 3.3.1 may become even more risky when a combination of anti-angiogenic and cytotoxic treatments is used (Fig. 9). The bistability observed for the virtual patient in Fig. 8 is present only for a narrow range of treatment scenarios. For a wide range of treatment scenarios, the singular strategy with zero resistance is evolutionarily repelling (Fig. 9c). The resistance strategy component then has a positive selection gradient, which leads to the emergence of treatment resistance even with small variations. Fig. 9b illustrates that increasing anti-angiogenic treatment may cause the average cancer population size to increase, due to the evolution of treatment resistance. Since high enough cytotoxic treatment does lead to non-viability of the cancer population, there may actually exist two different locally optimal treatment strategies: One option involves moderate cytotoxic and anti-angiogenic treatment levels, which do not remove the cancer population, but do not cause treatment resistance and have less side effects. The other option has just enough cytotoxic and anti-angiogenic treatment that the cancer population becomes non-viable even with treatment resistance. Comparing Fig. 8d and 9b we observe that despite the higher risk of resistance, the average population size achieved with the combination treatment is lower than that with the anti-angiogenic mono-therapy, even with low dosages that avoid the emergence of the anti-angiogenic treat-

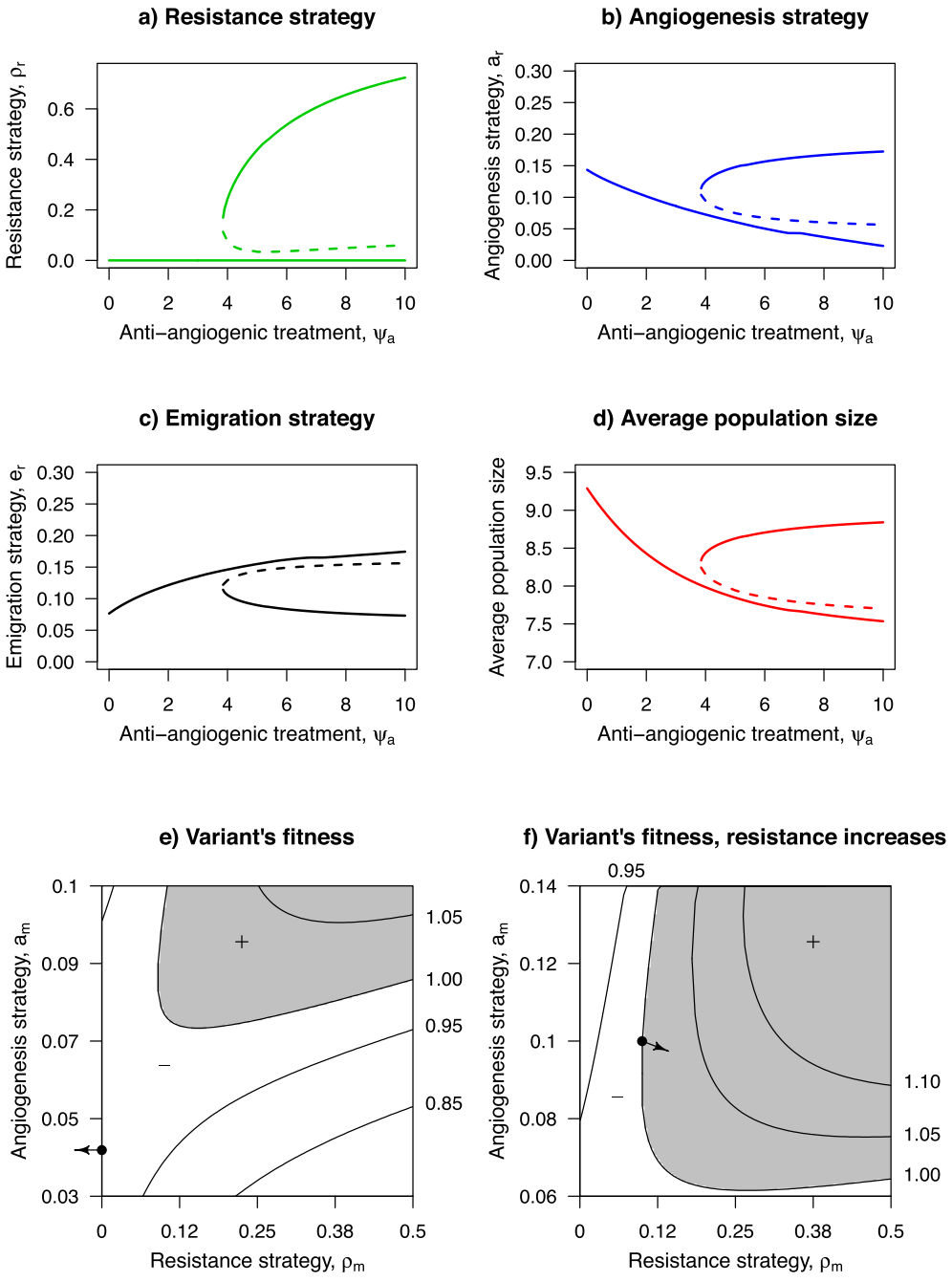


**Fig. 8.** Illustration of the singular strategies of the joint evolution of three strategy components: The a) resistance component, b) angiogenesis component and c) emigration component with respect to the anti-angiogenic treatment concentration $\psi_a$. The dashed line indicates the strategy components of the saddle point. d) The corresponding average population sizes. Panels e) and f) illustrate the variant's fitness landscape with respect to the variant's resistance strategy component and angiogenesis strategy component for two different resident strategies, e) $a_r \approx 0.043, e_r \approx 0.165$ and $\rho_r = 0$ and f) $a_r = e_r = \rho_r = 0.1$ (marked with a black dot in each panel), when $\psi_a = 7$. The resident strategy in panel e) is the singular strategy with $\rho_r = 0$. In each panel, the variant's emigration strategy is that of the resident, $e_m = e_r$. Contour curves with different fitness values (marked on the right side) are drawn in black. The black arrow points the direction of fitness gradient at the resident's strategy. Note that the resistance strategy component of the fitness gradient is positive in panel f). Here only anti-angiogenic mono-therapy is considered, thus $\psi_c = 0$. Other parameters are as in Table 1.

ment resistance. Interestingly, despite the full treatment resistance ($\rho_r = 1$), with the concentration of anti-angiogenic treatment above 1.4, the average population size stays lower than the average population size without the anti-angiogenic treatment. Thus, it seems that a combination treatment is preferable, even if the resistance to the anti-angiogenic treatment is obtained. However, as noted already in the previous section, the burden of two treatments might be intolerable for the patient.

In addition to treatments, the likelihood of resistance is also affected by the underlying biological parameters because each patient has their own unique biology which affects the cancer's conditions. So far we have investigated cancer development only with default parameter values presented in Table 1. We observed bistability with angiogenic monotherapy (Fig. 8). In addition to increasing cytotoxic treatment (Fig. 9), the scenario may shift with different parameters, such as by decreasing the resistance trade-off factor ($\beta$) (see Fig. 10 a vs. b), so that resistance will have a positive gradient from zero (Supplementary Fig. S9a). This will again lead into resistance more easily and with smaller treatment dose (see Supplementary Section 6). The treatment dosage is thus highly

sensitive and patient-specific when trying to avoid treatment resistance and simultaneously achieve sufficient treatment effect erasing the tumors.

## 4. Discussion

We have introduced a comprehensive metapopulation model for the cancer development considering three evolutionary strategies of cancer cells. These strategies include the contribution to angiogenesis, emigration and resistance to the anti-angiogenic treatment. Although angiogenesis and anti-angiogenic treatments have been modelled before (Nagy and Armbruster, 2012; Yonucu et al., 2017), to our knowledge, this is the first model that considers cancer microenvironment as a continuous-time metapopulation with an infinite number of patches where migration takes place through a dispersal pool. In addition to the anti-angiogenic therapy, we have modelled the cytotoxic treatment and investigated these two also as a combination therapy. The model provides insights into the development of cancer behavior and how the treatment interventions affect the outcome. It is shown that a positive angiogenesis contribution is often desirable for the cancer cells (when benefits outweigh the costs), similarly to the real-world observations where angiogenesis is required for tumor growth and metastases (Folkman, 1986; Liotta et al., 1974). It is also observed that the anti-angiogenic monotherapy does not typically eradicate the whole tumor. Eradication requires a combination with another treatment such as cytotoxic therapy (Alarcón et al., 2006; Lakka and Rao, 2008; Ribatti et al., 2019). The need for the cytotoxic treatment is reduced when used in a combination with the anti-angiogenic treatment. However, the side-effects and other costs may accumulate to an unbearable level if the regimens are chosen without careful consideration. In addition, the effect of anti-angiogenic treatment is compromised by the emergence of resistant variants. The model predicts that there is a patient-specific treatment threshold after which the resistance becomes

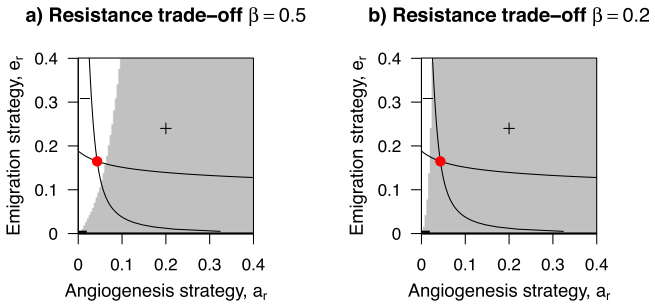


**Fig. 10.** The sign of resistance fitness gradient with respect to the angiogenesis and emigration strategies when the resistance strategy is set to zero and resistance trade-off is set to a) $\beta = 0.5$ or b) $\beta = 0.2$. Black curves indicate the zero-contours of angiogenesis and emigration fitness gradients with respect to each other. The singular strategies of the joint evolution of these two are at the intersections of the zero-contours (red dots). The concentration of anti-angiogenic treatment is set to 7 in panels a and b. Other parameters are as in Table 1.

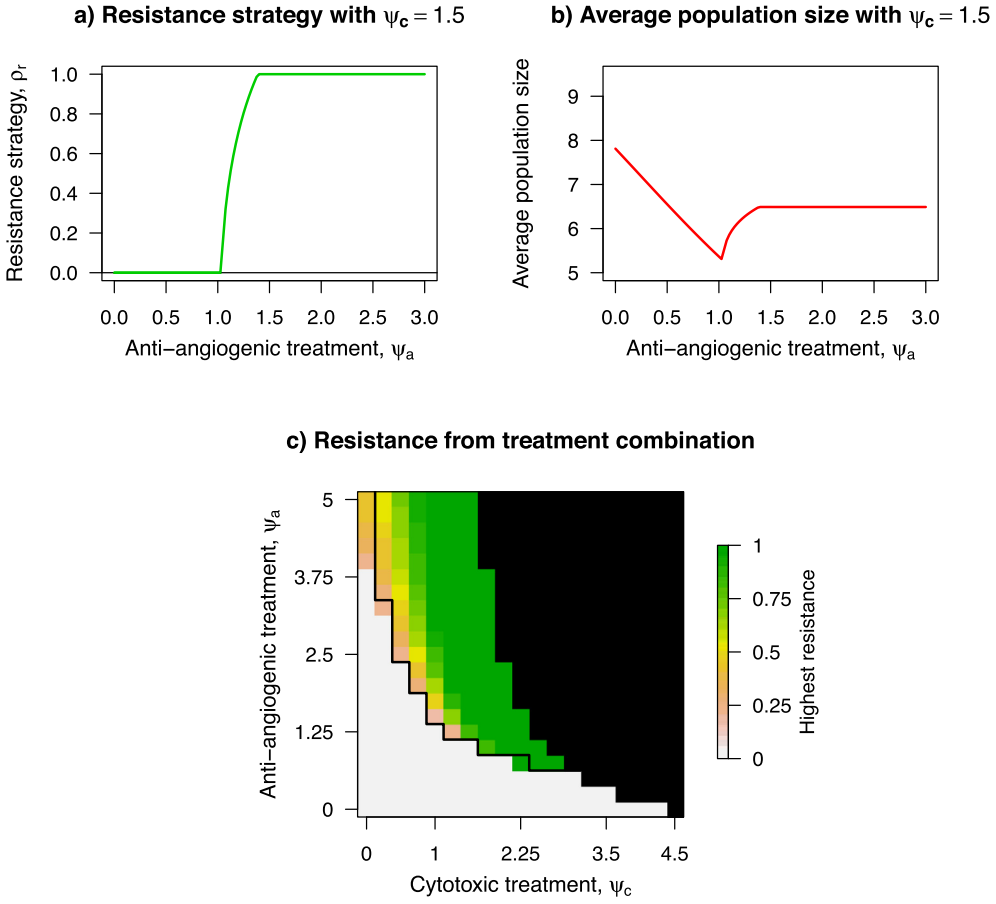


**Fig. 9.** a) The resistance strategy at the singular strategy of angiogenesis, emigration and resistance strategies with respect to the concentration of anti-angiogenic treatment when the effect of cytotoxic treatment is set to 1.5. b) The corresponding average population size. c) The resistance strategy in an evolutionarily attracting singular strategy with positive resistance component (highest resistance) with respect to anti-angiogenic and cytotoxic treatments. On the left side of the black line, the singular strategy with zero resistance is (additionally) attracting. Non-white color in this area denotes bistability. On the right side of the black line, the zero resistance is repelling. The black area denotes non-viability. Other parameters are as in Table 1.

profitable for the cancer cells. However, the positive treatment resistance is not self-evident in all cases and individual biological parameters determine how easily the resistance is acquired. Especially, the combination of anti-angiogenic and cytotoxic treatments enables the anti-angiogenic treatment resistance with higher likelihood than for the anti-angiogenic monotherapy. However, the combination treatment also results in better treatment effects, compared to monotherapies, even with the treatment resistance.

We analyzed systematically the effects of various treatment modalities as well as other biological parameters that affect the underlying cancer ecosystem dynamics. The effects were investigated using tools provided by adaptive dynamics (Brännström et al., 2013; Diekmann, 2003; Geritz et al., 1998). We calculated variant's metapopulation fitness to determine which strategies enable the variant's invasion to the resident population. For example, in the presence of anti-angiogenic treatment, a variant with lower angiogenesis strategy may have higher fitness compared to a resident that contributes more to the angiogenesis. In addition, the fitness gradient was calculated to determine in which direction the variant's fitness increases the most, which is the most likely direction of small variations. We assumed that all strategies are equally likely to variate. For example, the resistance strategy has a positive gradient in the setting of Fig. 8f, and this may lead into increased treatment resistance and lower treatment effect. The singular strategies were determined by the points in which the fitness gradients vanished. If attracting and invincible, the singular strategies determined where the dynamics would evolve in the current state of parameters. In addition, the average population sizes at the singular strategies were calculated to investigate how the tumor size is affected by changes in the cells' phenotypes.

Individual differences between patients' phenotypes and underlying biological parameters bring challenges to the modelling and investigation of the treatment responses. Furthermore, the mechanism of cancer development in itself is a complex process and, for simplicity, we assumed only a single angiogenesis mechanism. However, there exists multiple proangiogenic factors, e.g., VEGF family, fibroblast growth factors (FGFs) and platelet derived growth factors (PDGFs) (Khan and Bicknell, 2016). In future work, it would be interesting to include multiple angiogenesis mechanisms and the corresponding treatment options. In addition to angiogenesis, cancer may initiate also an immune response, which would be interesting addition to the model. This would also provide the possibility to include immunotherapy, which is an option for combination therapy with anti-angiogenic treatment (Khan and Kerbel, 2018; Lee et al., 2020). Another interesting option for future work is to consider the spatial location of the patches, because the travelled distance may affect the survival of emigrating cells, and local growth may be more common than distant metastases.

As noted above, cells and organisms are complex and their behavior is linked to many components and events in the microenvironment. This complicates the presentations of the ecosystem as a mathematical model. To avoid an over-complicated model, we had to make simplifications and assumptions (see Section 2). Especially, we omitted the endothelial cells and modelled only the resource inflow, which is assumed to be directly proportional to the number of endothelial cells. However, more endothelial cells do not necessary mean more resources or easier access as tumor vasculature tends to become distorted (Siemann, 2011). In the future work, it would be interesting to include the endothelial cells as an additional factor. In addition to resource inflow, changes in the vasculature may also affect the flow of drugs. In the current model, we assumed the treatment effect to be unaffected by fluctuations in the amount or normality of the veins. However, this is not the case in the actual system since there is evidence that anti-angiogenic treatment normalizes the vasculature, which then enables easier flow for drugs (Yonucu et al., 2017). In addition to omitting endothelial cells, we also limited the number of cancer cells in patches, as space limitations may hinder cell growth. This was done also partially for technical reasons, because the number of differential equations escalates when the maximum number of cells ($K$) increases. As a consequence, the computing times would also become infeasible. To prevent challenging and time-consuming analyses, we also considered only a monomorphic population with a single variant. In reality, there may be multiple competing cancer variants. However, this would dramatically increase the number of possible states in the Markov chain.

In the present work, we included the mechanisms that we deem to be the most prominent in the early cancer development. We included the main components of angiogenesis, anti-angiogenic treatment and the resistance to capture their principal effects. We hope that the model will bring valuable insights into the cancer development, angiogenesis and the anti-angiogenic treatment. Especially, the evident difficulties and modest responses to the anti-angiogenic treatments would benefit from additional knowledge as the angiogenesis remains as an important target for cancer treatment.

## Authors' contributions

ASH implemented the model, made the analyses and produced the figures. ASH and KP designed the study. ASH, KP and TA wrote the manuscript. KP and TA supervised the work.

## Funding

Academy of Finland (grants 313267 and 326238), Cancer Society of Finland, the Sigrid Jusélius Foundation, and University of Turku Graduate School (MATTI).

## CRediT authorship contribution statement

**Anni S. Halkola:** Conceptualization, Methodology, Software, Formal analysis, Writing – original draft, Writing – review & editing, Visualization. **Tero Aittokallio:** Writing – original draft, Writing – review & editing, Supervision. **Kalle Parvinen:** Conceptualization, Methodology, Validation, Writing – original draft, Writing – review & editing, Supervision.

## Declaration of Competing Interest

The authors declare that they have no known competing financial interests or personal relationships that could have appeared to influence the work reported in this paper.

## Appendix A. Supplementary data

Supplementary data associated with this article can be found, in the online version, athttps://doi.org/10.1016/j.jtbi.2022.111147.

## References

Alarcón, T., Owen, M.R., Byrne, H.M., Maini, P.K., 2006. Multiscale modelling of tumour growth and therapy: The influence of vessel normalisation on chemotherapy. Comput. Math. Methods Med. 7, 85–119. https://doi.org/10.1080/10273660600968994.

Avanzini, S., Antal, T., 2019. Cancer recurrence times from a branching process model. PLoS Comput. Biol. 15, 1–30. https://doi.org/10.1371/journal.pcbi.1007423.

Baffert, F., Thurston, G., Rochon-Duck, M., Le, T., Brekken, R., McDonald, D.M., 2004. Age-Related Changes in Vascular Endothelial Growth Factor Dependency and Angiopoietin-1-Induced Plasticity of Adult Blood Vessels. Circ. Res. 94, 984–992. https://doi.org/10.1161/01.RES.0000125295.43813.1F.

Benjamin, L.E., Keshet, E., 1997. Conditional switching of vascular endothelial growth factor (VEGF) expression in tumors: Induction of endothelial cell shedding and regression of hemangioblastoma-like vessels bv VEGF withdrawal. Proc. Natl. Acad. Sci. U.S.A. 94, 8761–8766. https://doi.org/10.1073/pnas.94.16.8761.

Bergers, G., Hanahan, D., 2008. Modes of resistance to anti-angiogenic therapy. Nat. Rev. Cancer 8, 592–603. https://doi.org/10.1038/nrc2442.

Bielenberg, D.R., Zetter, B.R., 2015. The Contribution of Angiogenesis to the Process of Metastasis. Cancer J. (United States) 21, 267–273. https://doi.org/10.1097/PPO.0000000000000138.

Bozic, I., Nowak, M.A., 2014. Timing and heterogeneity of mutations associated with drug resistance in metastatic cancers. Proc. Natl. Acad. Sci. 111, 15964–15968. https://doi.org/10.1073/pnas.1412075111.

Brännström, Å., Johansson, J., von Festenberg, N., 2013. The Hitchhiker's guide to adaptive dynamics. Games 4, 304–328. https://doi.org/10.3390/g4030304.

Comins, H.N., Hamilton, W.D., May, R.M., 1980. Evolutionarily stable dispersal strategies. J. Theor. Biol. 82, 205–230. https://doi.org/10.1016/0022-5193(80)90099-5.

Diekmann, O., 2003. A beginner's guide to adaptive dynamics. Banach Center Publications 63, 47–86. https://doi.org/10.4064/bc63-0-2.

Elice, F., Rodeghiero, F., 2012. PL-09 side effects of anti-angiogenic drugs. Thromb. Res. 129, S50–S53. https://doi.org/10.1016/S0049-3848(12)70016-6.

Fassoni, A.C., Roeder, I., Glauche, I., 2019. To Cure or Not to Cure: Consequences of Immunological Interactions in CML Treatment. Bull. Math. Biol. https://doi.org/10.1007/s11538-019-00608-x.

Fischer, A., Vázquez-García, I., Mustonen, V., 2015. The value of monitoring to control evolving populations. Proc. Natl. Acad. Sci. 112, 1007–1012. https://doi.org/10.1073/pnas.1409403112.

Folkman, J., 1986. How Is Blood Vessel Growth Regulated in Normal and Neoplastic Tissue?- G.H.A. Clowes Memorial Award Lecture. Cancer Res. 46, 467–473.

Frisch, S.M., Screaton, R.A., 2001. Anoikis mechanisms. Curr. Opin. Cell Biol. 13, 555–562. https://doi.org/10.1016/S0955-0674(00)00251-9.

Gandon, S., Michalakis, Y., 1999. Evolutionarily stable dispersal rate in a metapopulation with extinctions and kin competition. J. Theor. Biol. 199, 275–290. https://doi.org/10.1006/jtbi.1999.0960.

Gee, M.S., Procopio, W.N., Makonnen, S., Feldman, M.D., Yeilding, N.M., Lee, W.M., 2003. Tumor vessel development and maturation impose limits on the effectiveness of anti-vascular therapy. Am. J. Pathol. 162, 183–193. https://doi.org/10.1016/S0002-9440(10)63809-6.

Geritz, S.A., Kisdi, É., Meszéna, G., Metz, J.A., 1998. Evolutionarily singular strategies and the adaptive growth and branching of the evolutionary tree. Evol. Ecol. 12, 35–57. https://doi.org/10.1023/A:1006554906681.

Halkola, A.S., Parvinen, K., Kasanen, H., Mustjoki, S., Aittokallio, T., 2020. Modelling of killer T-cell and cancer cell subpopulation dynamics under immuno- and chemotherapies. J. Theor. Biol. 488, . https://doi.org/10.1016/j.jtbi.2019.110136 110136.

Heino, M., Hanski, I., 2001. Evolution of migration rate in a spatially realistic metapopulation model. Am. Naturalist 157, 495–511. https://doi.org/10.1086/319927.

Kemeny, J.G., Snell, J.L., 1960. Finite Markov chains. Princeton.

Khan, K.A., Bicknell, R., 2016. Anti-angiogenic alternatives to VEGF blockade. Clin. Exp. Metastasis 33, 197–210. https://doi.org/10.1007/s10585-015-9769-3.

Khan, K.A., Kerbel, R.S., 2018. Improving immunotherapy outcomes with anti-angiogenic treatments and vice versa. Nature Reviews. Clin. Oncol. 15, 310–324. https://doi.org/10.1038/nrclinonc.2018.9.

Komarova, N.L., Burger, J.A., Wodarz, D., 2014. Evolution of ibrutinib resistance in chronic lymphocytic leukemia (CLL). Proc. Natl. Acad. Sci. 111, 13906–13911. https://doi.org/10.1073/pnas.1409362111.

Kozłowska, E., Färkkilä, A., Vallius, T., Carpén, O., Kemppainen, J., Grénman, S., Lehtonen, R., Hynninen, J., Hietanen, S., Hautaniemi, S., 2018. Mathematical modeling predicts response to chemotherapy and drug combinations in ovarian cancer. Cancer Res. 78, 4036–4044. https://doi.org/10.1158/0008-5472.CAN-17-3746.

Lai, X., Geier, O.M., Fleischer, T., Garred, Ø., Borgen, E., Funke, S.W., Kumar, S., Rognes, M.E., Seierstad, T., Børresen-Dale, A.L., Kristensen, V.N., Engebråten, O., Köhn-Luque, A., Frigessi, A., 2019. Towards personalized computer simulation of breast cancer treatment: a multi-scale pharmacokinetic and pharmacodynamic model informed by multi-type patient data. Cancer Res. https://doi.org/10.1158/0008-5472.CAN-18-1804.

Lakka, S.S., Rao, J.S., 2008. Antiangiogenic therapy in brain tumors. Expert Rev. Neurotherap. 8, 1457–1473. https://doi.org/10.1586/14737175.8.10.1457.

Lee, W.S., Yang, H., Chon, H.J., Kim, C., 2020. Combination of anti-angiogenic therapy and immune checkpoint blockade normalizes vascular-immune crosstalk to potentiate cancer immunity. Exp. Mol. Med. 52, 1475–1485. https://doi.org/10.1038/s12276-020-00500-y.

Letellier, C., Sasmal, S.K., Draghi, C., Denis, F., Ghosh, D., 2017. A chemotherapy combined with an anti-angiogenic drug applied to a cancer model including angiogenesis. Chaos Solitons Fractals 99, 297–311. https://doi.org/10.1016/j.chaos.2017.04.013.

Liotta, L.A., Kleinerman, J., Saidel, G.M., 1974. Quantitative Relationships of Intravascular Tumor Cells, Tumor Vessels, and Pulmonary Metastases following Tumor Implantation. Cancer Res. 34, 997–1004.

Melnyk, O., Kim, K.J., Shuman, M.A., 1996. Vascular Endothelial Growth Factor Promotes Tumor Dissemination by a Mechanism Distinct from Its Effect on Primary Tumor Growth. Cancer Res. 56, 921–924.

Metz, J.A., Gyllenberg, M., 2001. How should we define fitness in structured metapopulation models? Including an application to the calculation of evolutionarily stable dispersal strategies. Proc. R. Soc. B: Biol. Sci. 268, 499–508. https://doi.org/10.1098/rspb.2000.1373.

Metz, J.A.J., Geritz, S.A.H., Metz, A., Nisbet, R.M., 1992. How Should We Define 'Fitness' for General Ecological Scenarios? The simplest textbook model for selection in large populations relies N(t fl) = B(E(t)) N(t) (1) with B(E(t)) a matrix whose el-ements depend on E(t), implying N(t) = B(E(I-I)) B(E(t-2)). Trends Ecol. Evol. 7, 198–202.

Nagy, J.D., Armbruster, D., 2012. Evolution of uncontrolled proliferation and the angiogenic switch in cancer. Math. Biosci. Eng. 9, 843–876. https://doi.org/10.3934/mbe.2012.9.843.

Parvinen, K., 2011. Adaptive Dynamics of Altruistic Cooperation in a Metapopulation: Evolutionary Emergence of Cooperators and Defectors or Evolutionary Suicide? Bull. Math. Biol. 73, 2605–2626. https://doi.org/10.1007/s11538-011-9638-4.

Parvinen, K., Metz, J.A., 2008. A novel fitness proxy in structured locally finite metapopulations with diploid genetics, with an application to dispersal evolution. Theor. Popul. Biol. 73, 517–528. https://doi.org/10.1016/j.tpb.2008.01.002.

Pinho, S.T., Bacelar, F.S., Andrade, R.F., Freedman, H.I., 2013. A mathematical model for the effect of anti-angiogenic therapy in the treatment of cancer tumours by chemotherapy. Nonlinear Anal.: Real World Appl. 14, 815–828. https://doi.org/10.1016/j.nonrwa.2012.07.034.

Qiao, L., Farrell, G.C., 1999. The effects of cell density, attachment substratum and dexamethasone on spontaneous apoptosis of rat hepatocytes in primary culture. In Vitro Cellular Develop. Biol. - Animal 35, 417–424. https://doi.org/10.1007/s11626-999-0117-2.

Rajabi, M., Mousa, S.A., 2017. The role of angiogenesis in cancer treatment. Biomedicines 5. https://doi.org/10.3390/biomedicines5020034.

Ramjiawan, R.R., Griffioen, A.W., Duda, D.G., 2017. Anti-angiogenesis for cancer revisited: Is there a role for combinations with immunotherapy? Angiogenesis 20, 185–204. https://doi.org/10.1007/s10456-017-9552-y.

Ribatti, D., Annese, T., Ruggieri, S., Tamma, R., Crivellato, E., 2019. Limitations of Anti-Angiogenic Treatment of Tumors. Transl. Oncol. 12, 981–986. https://doi.org/10.1016/j.tranon.2019.04.022.

Robert, N.J., Diéras, V., Glaspy, J., Brufsky, A.M., Bondarenko, I., Lipatov, O.N., Perez, E. A., Yardley, D.A., Chan, S.Y., Zhou, X., Phan, S.C., O'Shaughnessy, J., 2011. RIBBON-1: Randomized, double-blind, placebo-controlled, phase III trial of chemotherapy with or without bevacizumab for first-line treatment of human epidermal growth factor receptor 2-negative, locally recurrent or metastatic breast cancer. J. Clin. Oncol. 29, 1252–1260. https://doi.org/10.1200/JCO.2010.28.0982.

Rowe, D.H., Huang, J., Kayton, M.L., Thompson, R., Troxel, A., O'Toole, K.M., Yamashiro, D., Stolar, C.J., Kandel, J.J., 2000. Anti-VEGF antibody suppresses primary tumor growth and metastasis in an experimental model of Wilms' tumor. J. Pediatr. Surg. 35, 30–33. https://doi.org/10.1016/S0022-3468(00)80008-1.

Saif, M.W., Elfiky, A., Salem, R.R., 2007. Gastrointestinal perforation due to bevacizumab in colorectal cancer. Ann. Surg. Oncol. 14, 1860–1869. https://doi.org/10.1245/s10434-006-9337-9.

Shaheen, R.M., Davis, D.W., Liu, W., Zebrowski, B.K., Wilson, M.R., Bucana, C.D., McConkey, D.J., McMahon, G., Ellis, L.M., 1999. Antiangiogenic therapy targeting the tyrosine kinase receptor for vascular endothelial growth factor receptor inhibits the growth of colon cancer liver metastasis and induces tumor and endothelial cell apoptosis. Cancer Res. 59, 5412–5416.

Siemann, D.W., 2011. The Unique Characteristics of Tumor Vasculature and Preclinical Evidence for its Selective Disruption by Tumor-Vascular Disrupting Agents. Cancer Treat. Rev. 37, 63–74. https://doi.org/10.1016/j.ctrv.2010.05.001.

Smith, H.L., Waltman, P.E., 1995. The theory of the chemostat: dynamics of microbial competition. Cambridge University Press.

Takahashi, Y., Kitadai, Y., Bucana, C.D., Ellis, L.M., Takahashi, Y., Ellis, L.M., Cleary, K. R., 1995. Expression of Vascular Endothelial Growth Factor and Its Receptor, KDR, Correlates with Vascularity, Metastasis, and Proliferation of Human Colon Cancer. Cancer Res. 55, 3969–3972.

Tiwari, N., Gheldof, A., Tatari, M., Christofori, G., 2012. EMT as the ultimate survival mechanism of cancer cells. Semin. Cancer Biol. 22, 194–207. https://doi.org/10.1016/j.semcancer.2012.02.013.

Tóth, P., Érdi, J., 1989. Mathematical Models of Chemical Reactions: Theory and Applications of Deterministic and Stochastic Models. Manchester University Press.

Truelsen, S.L.B., Mousavi, N., Wei, H., Harvey, L., Stausholm, R., Spillum, E., Hagel, G., Qvortrup, K., Thastrup, O., Harling, H., Mellor, H., Thastrup, J., 2021. The cancer angiogenesis co-culture assay: In vitro quantification of the angiogenic potential of tumoroids. PLoS ONE 16, 1–22. https://doi.org/10.1371/journal.pone.0253258.

Vasudev, N.S., Reynolds, A.R., 2014. Anti-angiogenic therapy for cancer: Current progress, unresolved questions and future directions. Angiogenesis 17, 471–494. https://doi.org/10.1007/s10456-014-9420-y.

Wang, H., Vo, T., Hajar, A., Li, S., Chen, X., Parissenti, A.M., Brindley, D.N., Wang, Z., 2014. Multiple mechanisms underlying acquired resistance to taxanes in selected docetaxel-resistant MCF-7 breast cancer cells. BMC Cancer 14. https://doi.org/10.1186/1471-2407-14-37.

Wang, R.C., Chen, X., Parissenti, A.M., Joy, A.A., Tuszynski, J., Brindley, D.N., Wang, Z., 2017. Sensitivity of docetaxel-resistant MCF-7 breast cancer cells to

microtubule-destabilizing agents including vinca alkaloids and colchicine-site binding agents. PLoS ONE 12, 1–22. https://doi.org/10.1371/journal.pone.0182400.

Warren, R.S., Yuan, H., Matli, M.R., Gillett, N.A., Ferrara, N., 1995. Regulation by vascular endothelial growth factor of human colon cancer tumorigenesis in a mouse model of experimental liver metastasis. J. Clin. Invest. 95, 1789–1797. https://doi.org/10.1172/JCI117857.

Yonucu, S., Yılmaz, D., Phipps, C., Unlu, M.B., Kohandel, M., 2017. Quantifying the effects of antiangiogenic and chemotherapy drug combinations on drug delivery and treatment efficacy. PLoS Comput. Biol. 13, 1–17. doi: 10.1371/journal.pcbi.1005724..

Zhang, J., Cunningham, J.J., Brown, J.S., Gatenby, R.A., 2017. Integrating evolutionary dynamics into treatment of metastatic castrate-resistant prostate cancer. Nat. Commun. 8, 1–10. https://doi.org/10.1038/s41467-017-01968-5.